GEOPHYSICAL RESEARCH LETTERS, VOL. 28, NO. 7, PAGES 1331-1334, APRIL 1, 2001

Rapid aseismic moment release following the 5 December, 1997 Kronotsky, Kamchatka, earthquake

R. Bürgmann,[1] M. G. Kogan,[2] V. E. Levin,[3] C. H. Scholz,[2] R. W. King,[4] and G. M. Steblov[5]

Abstract. Model inversions of displacements of continuously operating GPS stations in Kamchatka show that aseismic afterslip during 2 months following the M_w=7.8, 5 December, 1997 Kronotsky subduction earthquake released as much moment as the earthquake itself. The rapidly decaying transient slip on the subduction underthrust occurred near the downdip edge of the coseismic rupture and extended laterally away from it, including a region of vigorous foreshock activity. A logarithmic decay function fit to the cumulative afterslip curve has a relaxation time of about 3 days. Rapid afterslip can contribute significantly to the moment release of partially coupled subduction zones.

Introduction

To better determine the seismic potential of subduction zones, it is important to understand the spatial and temporal distribution of elastic strain accumulation and release of the plate boundary underthrust. Interseismic deformation measurements along subduction zones throughout the world reveal varying degrees of locking of the plate-interface faults, ranging from complete locking over great width to freely creeping segments. However, even a subduction zone that appears completely locked for long periods of time might accommodate significant amounts of slip by aseismic episodic slip events such as slow earthquakes and postseismic afterslip [*Heki et al.*, 1997; *Mazzotti et al.*, 2000].

The occurrence of aseismic slip can be time-dependent at various time scales and is not always directly related to preceding large earthquakes. *Heki et al.* [1997] found that rapid deformation over the first year following a 1994 subduction earthquake in northeastern Japan was due to continued aseismic slip on or near the coseismic rupture. *Hirose et al.* [1999] found afterslip following two moderate subduction earthquakes in southwestern Japan, which were followed a few months later by a separate slow slip event of comparable moment about 200 km north of the epicenters. Here we investigate time-dependent deformation captured by continuous GPS observations along the Kamchatka subduction zone, which show a phase of rapid aseismic afterslip during 2 months following the Kronotsky earthquake. Displacements during this time were comparable in size with the coseismic motions and their rapid decay suggests that the deformation was due to afterslip rather than viscous relaxation processes, which take place on time scales of years and decades [*Thatcher*, 1986].

The Kronotsky Earthquake

Several large subduction zone earthquakes have occurred along the Kamchatka arc, including major ruptures in 1923 (M_s = 8.1), 1952 (M_w = 9.0), 1959 (M_s = 8.2) and 1971 (M_s = 8.0) (Fig. 1A). Historically, the Kamchatka subduc-

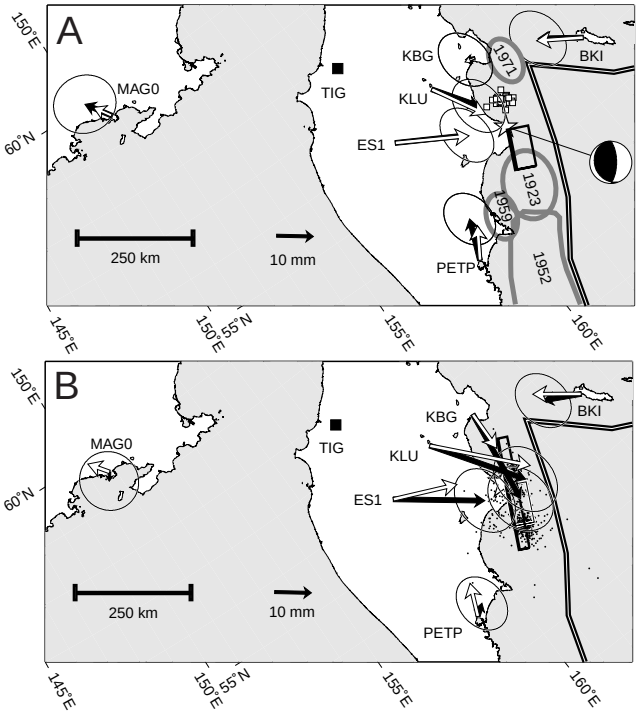

Figure 1. (A) Coseismic GPS displacements relative to TIG (filled arrows with 95% confidence ellipses from difference of Dec. 4 24-hr and Dec. 5 noon-to-midnight solutions). Predicted displacements (white open arrows) are from dislocation model B_{cos} in Table 1. The surface projection of the model fault is shown as a bold rectangle to the south of the main shock (star) and the foreshock sequence (open squares). Aftershock zones of great 20th century earthquakes [*Fedotov et al.*, 1999] are outlined with gray lines. The map is drawn in an oblique Mercator projection, where horizontal lines and station motions are aligned parallel to relative Pacific - North America plate motion. (B) Displacements during 56 days following the earthquake (filled arrows) and fit from postseismic dislocation model (open arrows from model B_{post} in Table 1). Bold rectangle is the postseismic dislocation and the thin-lined rectangle is the coseismic model from (A). Black dots are aftershocks through January 1998.

[1]Department of Earth and Planetary Science, University of California, Berkeley, California
[2]Lamont-Doherty Earth Observatory, Palisades, New York
[3]Kamchatka GPS Center KOMSP, Petropavlovsk, Russia
[4]Department of Earth, Atmospheric, and Planetary Sciences, Massachusetts Institute of Technology, Cambridge, Massachusetts
[5]DAAC GSRAS, Moscow, Russia

Paper number 2000GL012350.
0094-8276/01/2000GL012350$05.00

Table 1. Parameters for geodetically determined fault models from inversion of coseismic and 56-day postseismic GPS data and coseismic fault parameters from seismologic studies

	Length (km)	Width (km)	Depth (km)	Dip (°W)	Strike (°)	Lat. (°)	Lon. (°)	Slip (m ± 1 σ)	$WRSS$	Misfit	Mo (Nm×10^{20})	M_w
A_{cos}	*90*	*50*	58.5	28.4	27.0	54.19	162.57	2.81 ± 0.19	5.2	0.31	3.8	7.7
B_{cos}	*90*	*50*	*30*	19.0	27.7	54.23	162.33	3.02 ± 0.20	6.0	0.35	4.1	7.7
A_{post}	*90*	*50*	*30*	*19.0*	*27.7*	*54.23*	*162.33*	3.27 ± 0.24	64.1	3.77	4.4	7.8
B_{post}	248	*25*	41	*19.0*	*27.7*	54.51	162.24	1.93 ± 0.13	25.9	1.53	3.6	7.7
Sohn, 1998	88		30	24.4	43.7	54.90	162.11				2.5	7.6
Harvard CMT			29	23	22	54.31	161.91				5.3	7.8

Numbers in italics are constrained, rather than solved for in the inversion. $WRSS$ is weighted residual sum of squares and misfit is $\sqrt{WRSS/(N-P)}$, where N is the number of data and P is the number of free model parameters. Latitude and longitude refer to the center of upper dislocation edge, and depth is to the dislocation center or to the moment tensor centroid.

tion zone appears fully coupled south of 53°N (dominantly breaking in 1952-type earthquakes), and only 40-50% coupled along the northern portion of the arc [*Pacheco et al.*, 1993]. At 11:26 GMT, on 5 December, 1997, the M_w = 7.8 Kronotsky earthquake ruptured the plate interface, just north of the epicentral region of the 1923 event [*Fedotov et al.*, 1999; *Gordeev et al.*, 1999]. Analysis of teleseismic waveforms [*Sohn*, 1998] revealed that the earthquake occurred on a ∼24° northwest-dipping fault plane at ∼30 km depth and propagated from the hypocenter towards the southwest for ∼90 km (Table 1).

The Kronotsky earthquake was preceded by a swarm of foreshocks (Fig. 1A), which commenced 49 hours before the main shock and included 34 $m_b \geq 4$ events just north of the hypocenter. The largest foreshock (M_w = 5.5) occurred 3 hours prior to the main event and had a similar 22°-northwest-dipping focal mechanism nodal plane. Aftershocks occurred over a ∼200- km wide zone with a dense cluster of events to the southwest; however, aftershocks are notably absent in the area of foreshock activity (Fig. 1B). The average dip of the northwest-dipping nodal planes of foreshocks and aftershocks [*Dziewonski et al.*, 1998] is 28 degrees, which is consistent with the main-shock geometry and constraints on the subduction zone geometry from background seismicity [*Pacheco et al.*, 1993; *Gorbatov et al.*, 1997]. *Gorbatov et al.* [1997] estimate the depth to the plate interface near the hypocenter at ∼40 km, somewhat deeper than indicated by the seismic inversions (Table 1).

GPS Measurements and Models of Coseismic and Postseismic Deformation

We analyzed in 24-hr solutions phase data from seven continuously operating GPS stations in Kamchatka, eastern Siberia, and on Bering Island. We then combined the estimated station positions for each day with a similar analysis of global data performed by the Scripps Orbital and Permanent Array Center (SOPAC) and expressed these positions in a North American reference frame, as described by *Kogan et al.* [2000]. The site motions caused by the Kronotsky earthquake and subsequent rapid postseismic deformation are shown relative to Tigil (TIG) in western Kamchatka in Fig. 1 and Fig. 2. We find no resolvable pre-earthquake station displacements associated with the 49-hr foreshock sequence (Fig. 2). None of the stations had significant vertical displacements, but all components are included in the modeling of coseismic and postseismic deformation.

The time series (Fig. 2) show rapid transient deformation immediately following the Kronotsky earthquake. Fig. 1B shows the postseismic displacements of the first 56 days following the event (from noon of 97/12/05 to 98/01/30). KLU and ES1 continued to move towards the southeast, with the motion of KLU being more than twice its coseismic offset. PETP did not move following its ∼10 mm coseismic offset. The station velocities decayed to significantly lower rates by the end of 1997 (Fig. 2). Station KBG had insignificant coseismic displacements and showed no postseismic motions until 10 December, when it started to move rapidly towards the south. However, this station suffered from repeated receiver problems during this time period, complicating the interpretation of the data from this site. While the postseismic deformation of the first 2 months roughly resembles the coseismic motions and is of comparable magnitude (Fig. 1), the differences described above and their development in time suggest spatio-temporal complexity in the postseismic deformation.

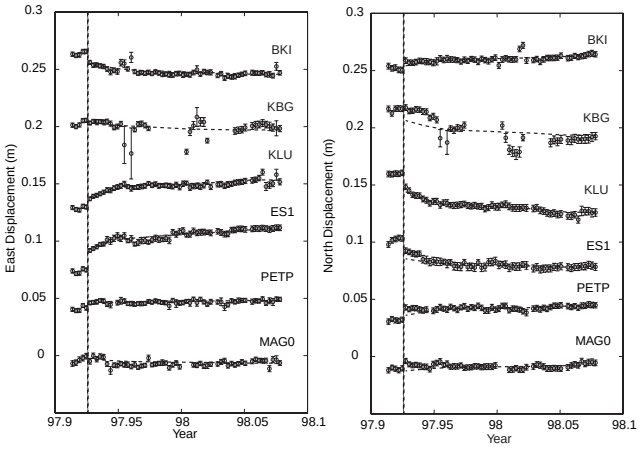

Figure 2. Time series of East (left panel) and North (right panel) coordinate components relative to station TIG (Fig. 1) from 97/12/05 to 98/01/30. Vertical line indicates time of Kronotsky earthquake. Dashed bold line starting at the time of the main shock indicates predicted displacements from time-dependent model inversion of the postseismic GPS data. Individual time series are offset for clarity.

The sparse GPS network allows us to only address simple first-order models of the deformation. We model the observed coseismic displacements and subsequent rapid transient deformation using rectangular, uniform-slip dislocations in an elastic half-space [*Okada*, 1985]. To find the geometry of the coseismic rupture and postseismic afterslip plane, we use a constrained, nonlinear optimization algorithm [*Bürgmann et al.*, 1997]. The inversion determines the best-fit geometry (parameterized by length, depth, width, dip, strike, and location) and the amount of slip (dip slip only) of the dislocation. Our inversions seek to minimize the weighted residual sum of squares $WRSS = (d_{obs} - d_{mod})^{\mathrm{T}} \times cov^{-1} \times (d_{obs} - d_{mod})$, where d_{obs} and d_{mod} are the observed and modeled motions relative to TIG, respectively, and *cov* is the full data covariance matrix that accounts for correlations between the three displacement components of all stations. We choose TIG as the reference site because it is centrally located, has a relatively low scatter relative to the ten stations that define the North American reference frame, and has been consistently observed throughout the time period. We apply constraints on some of the fault-geometry parameters in the inversions to find a model rupture that is consistent with inversions of mainshock seismograms [*Sohn*, 1998], the distribution of aftershocks, and the geometry of the plate interface based on studies of the pre-earthquake seismicity [*Gorbatov et al.*, 1997]. We adopt the rupture length of 90 km from *Sohn* [1998] and assign a down-dip rupture width of 50 km consistent with the distribution of aftershocks.

Without any additional constraints, our best-fitting model dislocation (A_{cos} in Table 1) lies within the zone of aftershocks southeast of the hypocenter, but is located deeper (58 km) than the seismic moment centroid depth (30 km, Sohn 1998) and estimates of the depth to the plate interface (∼40 km, Gorbatov et al., 1997). If we constrain the center of the fault to lie at 30-km depth, we find a model with similar geometry and moment and insignificantly increased misfit (B_{cos} in Table 1). We find that the geodetic data are consistent with rupture parameters determined from seismic data and indicate a coseismic moment release of $\sim 4 \times 10^{20}$ Nm corresponding to a $M_w = 7.7$.

Continued uniform slip on the rupture plane does not provide a good fit to the postseismic displacements (model A_{post} in Table 1). If we fix the strike and dip of the afterslip plane to that of the coseismic rupture, the geometry inversion finds a significantly better-fitting model that is located near the bottom edge of the rupture and extends laterally beyond the coseismic fault plane (B_{post} in Table 1). The afterslip fault plane includes the area of vigorous foreshock activity during three days before the main event (Fig. 1A). The lateral extent of the afterslip plane in the north is mainly determined by station KBG. The delayed postseismic response of this station suggests that afterslip in the north initiated after several days. The postseismic motions are difficult to fit with a single dislocation plane, but the sparcity of stations does not permit more complex slip-distributed models or multiple fault planes.

Aseismic Moment Release Following the Kronotsky Earthquake

We compare the seismic moment of aftershocks to the moment release deduced from model inversions of the time-dependent GPS-station displacements in the two months following the Kronotsky earthquake (Fig. 3). The moment associated with fault slip is $M_o = \mu \times A \times u$, where μ is the crustal rigidity (taken to be 30 GPa), A is the surface area of the fault, and u is the fault slip. The seismic moments of the aftershock sequence are derived from the Harvard CMT catalog [*Dziewonski et al.*, 1998] of $5 \leq M_w \leq 6.5$ events in the epicentral region. Events smaller than the detection threshold could increase the total seismic moment release estimate by ∼10%, assuming a b-value of 1 in the Gutenberg-Richter, magnitude-frequency relationship.

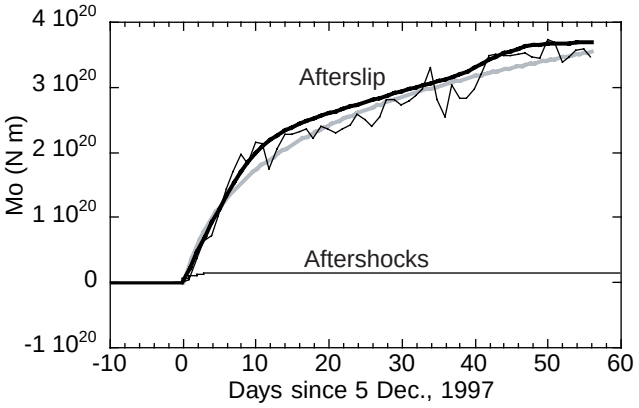

Figure 3. Cumulative seismic moment released in Kronotsky-earthquake aftershocks (thin black line) compared to time-dependent postseismic moment determined from network-inversion-filter afterslip model of daily GPS solutions. Bold black line: temporal smoothing factor chosen to ensure all slip is in thrust sense. Thin line: no smoothing. Predicted motions from the smoothed model are shown in Fig. 2. Bold gray line is logarithmic line fit to the unsmoothed slip function with a relaxation time of 3 days.

We use the Network Inversion Filter developed by *Segall and Matthews* [1997; *Segall et al.*, 2000] to determine the temporal character of moment released by afterslip constrained by 56 daily GPS solutions of the post-earthquake period. The observed position changes are assumed to result from temporally varying dip slip on the dislocation plane determined in the geometry inversion (model B_{post} in Table 1) and from random walk noise (2 mm $\mathrm{yr}^{-1/2}$). The random walk component accounts for any errors with correlation times greater than one day, such as benchmark instability and atmospheric or GPS satellite orbital errors. Thus, we make no assumption about the governing form (logarithmic or exponential) of the transient, but constrain the model directly with the daily GPS solutions shown in Fig. 2. We determine the amount of temporal smoothing [*Segall et al.*, 2000] by choosing the smallest smoothing parameter that ensures that no normal slip occurs throughout the time period. We invert for the time-dependent afterslip rate on the model fault shown in Fig. 1B from which we derive the cumulative moment release (Fig. 3). The predicted displacements from this model fit the observed position changes well (dashed lines in Fig. 2) except for the motions at KBG. The final cumulative slip (2.02 m) and moment (3.7×10^{20} Nm) determined using the network inversion filter are close to those found from the inversion of displacements between 97/12/05 and 98/01/30 (Table 1). The moment released by rapidly decaying afterslip during the first 2 months fol-

lowing the Kronotsky earthquake is approximately equal to that released during the earthquake.

Discussion and Conclusions

Rate and state variable friction laws applied to afterslip suggest that slip decays logarithmically [*Marone et al.*, 1991]. We fit the cumulative afterslip curve to the logarithmic two-parameter expression, $u = \alpha * ln(\beta t + 1)$ [*Heki et al.*, 1997], where u is accumulated fault slip at time t and α and β are model variables that can be related to friction law parameters. The predicted moment release from the best-fit logarithmic slip decay curve has a β of 0.32 days^{-1} corresponding to a logarithmic relaxation time $1/\beta$ of ~3 days (Fig. 3). The afterslip decayed to near zero rates within the 2-month period we discuss here. In the four subsequent months, additional motions of ES1 and KLU, which define the transient deformation are only about 4 and 7 mm, respectively.

Motions of GPS sites near the Kronotsky earthquake show that $\sim 3.7 \times 10^{20}$ Nm were released aseismically during a phase of rapidly decaying afterslip, comparable to the coseismic moment. As *Heki et al.* [1997] report for Japan, we find that aseismic afterslip can account for a significant amount of plate interface slip along the partially coupled portion of the Kamchatka subduction zone. The model inversions are consistent with afterslip on velocity-strengthening portions of the plate interface adjacent to the asperity that dynamically ruptured in the earthquake, but some of the afterslip might well occur on the coseismic rupture itself. The afterslip apparently includes the zone of foreshock activity, which might have been associated with a small amount of slow slip preceding the mainshock. Significant aseismic moment release helps explain the sometimes large discrepancy between estimates of the seismic moment expected from plate convergence rates and the moment released in historic subduction-zone earthquakes.

Acknowledgments. Seismic locations shown in Figure 1 are from the Council of the National Seismic System (CNSS) catalog archived at the Northern California Earthquake Data Center (NCEDC). Figure 1 was drawn with the GMT software [Wessel and Smith, 1995]. We thank Rachel Abercombie for discussions and valuable comments on the manuscript. Funding for this research provided by NSF grant EAR-9814784 to LDEO and MIT.

References

Bürgmann, R., P. Segall, M. Lisowski, and J. Svarc, Postseismic strain following the 1989 Loma Prieta earthquake from GPS and leveling measurements, *J. Geophys. Res., 102*, 4933-4955, 1997.

Dziewonski, A.M., G. Ekström, and N.N. Maternovskaya, Centroid-moment tensor solutions for October-December, 1997, Phys. Earth Planet. Int., *109*, 93-105, 1998.

Fedotov, S.A., S.D. Chernyshev, Y.D. Matvienko, and N.A. Zharinov, The forecast of the December 5, 1997, magnitude 7.8-7.9 Kronotsky earthquake, Kamchatka, and its M=6 aftershocks, Volc. Seis., *20*, 597-613, 1999.

Gorbatov, A., V. Kostoglodov, G. Suarez, and E. Gordeev, Seismicity and structure of the Kamchatka subduction zone, *J. Geophys. Res., 102*, 17883-17898, 1997.

Gordeev, E., V. Levin, M. Kasahara, V. Bakhtiarov, V. Chebrov, and M. Maguskin, GPS monitoring in Kuril-Kamchatka and Aleutian arcs junction, Eos Trans. AGU, *80*, 948, 1999.

Heki, K., S. Miyazaki, and H. Tsuji, Silent fault slip following an interplate thrust earthquake at the Japan trench, Nature, *386*, 595-598, 1997.

Hirose, J., K. Hirahara, F. Kimata, N. Fjii, and S. Miyazaki, A slow thrust slip event following the two 1996 Hyuganada earthquakes beneath the Bongo Channel, southwest Japan, *Geophys. Res. Lett., 26*, 3237-3240, 1999.

Kogan, M.G., G.M. Steblov, R.W. King, T.A. Herring, D.I. Frolov, S.G. Egorov, V.Y. Levin, A. Lerner-Lam, and A. Jones, Geodetic constraints on the relative motion and rigidity of Eurasia and North America, *Geophys. Res. Lett., 27*, 2041-2044, 2000.

Marone, C.J., C.H. Scholz, and R.G. Bilham, On the mechanics of earthquake afterslip, *J. Geophys. Res., 96*, 8441-8452, 1991.

Mazzotti, S., X. Le Pichon, and P. Henry, Full interseismic locking of the Nankai and Japan-west Kurile subduction zones: An analysis of uniform elastic strain accumulation in Japan constrained by permanent GPS, *J. Geophys. Res., 105*, 13159-13177, 2000.

Okada, Y., Surface deformation due to shear and tensile faults in a half-space, *Bull. Seismol. Soc. Am., 75*, 1135-1154, 1985.

Pacheco, J.F., L.R. Sykes, and C.H. Scholz, Nature of seismic coupling along simple plate boundaries of the subduction type, *J. Geophys. Res., 98*, 14133-14159, 1993.

Segall, P., R. Bürgmann, and M. Matthews, Time dependent deformation following the 1989 Loma Prieta earthquake, *J. Geophys. Res., 105*, 5615-5634, 2000.

Segall, P., and M. Matthews, Time dependent inversion of geodetic data, *J. Geophys. Res., 103*, 22,391-22,409, 1997.

Sohn, S.W., The 1997 Kamchatka earthquake, ISEIAM, *34*, 91-99, 1998.

Thatcher, W., Cyclic deformation related to great earthquakes at plate boundaries, Royal Soc. New Zealand Bull., *24*, 245-272, 1986.

Wessel, P., and W.H.F. Smith, New version of the Generic Mapping Tools released, EOS, Trans. Amer. Geophys. U., *76*, 329, 1995.

R. Bürgmann, Dept. of Earth and Planetary Science, 307 McCone Hall, University of California, Berkeley, Berkeley, CA 94720 (e-mail: burgmann@seismo.berkeley.edu)

M. G. Kogan, C. H. Scholz, Lamont-Doherty Earth Observatory, Palisades, NY 10964

R. W. King, Department of Earth, Atmospheric, and Planetary Sciences, Massachusetts Institute of Technology, Cambridge, MA 02139

V. E. Levin, Kamchatka GPS Center KOMSP, Petropavlovsk, Russia

G. M. Steblov, DAAC GSRAS, Moscow, Russia

(Received September 18, 2000; revised November 9, 2000; accepted November 16, 2000.)